γ

UCRL - 75878
PREPRINT
Conf - 741079 - - 9

LAWRENCE LIVERMORE LABORATORY
University of California/Livermore, California

COMPUTER SIMULATIONS OF LASER DRIVEN IMPLOSION OF SEEDED HOLLOW PELLETS

J. T. Larsen

October 28, 1974

This paper was prepared for the 16th Annual Meeting of Division of Plasma Physics of the Ammerican Physics Society on
October 28-31, 1974
Albuquerque, New Mexico

COMPUTER SIMULATIONS OF LASER DRIVEN

IMPLOSION OF SEEDED HOLLOW PELLETS *

J. T. Larsen

INTRODUCTION

In a paper presented last year in Philadelphia, Lindl[1] investigated the effect of a superthermal electron tail on a solid DT sphere imploded with a shaped laser pulse. His results have provided the motivation and direction for this paper.

Laser light is absorbed in a plasma by inverse bremsstrahlung, plasma decay instabilities and resonance absorption processes. Of these processes, inverse bremsstrahlung is the most important at low laser powers and results in a near Maxwellian distribution of electrons. As the laser power is increased the plasma instabilities and resonant absorption modes become important resulting in a significant number of electrons having temperatures far above that of a thermal (Maxwellian) distribution. These hot, energetic electrons outside the critical radius for light absorption do not couple well to those cooler electrons inside because of the long mean-free-path. Hence these energetic electrons deposit their energy deep within the pellet and result in preheating of the DT fuel. Figure 1 shows this in terms of the adiabat along which the compression takes place. The effect of the hot electrons is to move to a higher adiabat thus requiring more driving pressure to achieve the desired compression. In

*Research performed under the auspices of the U. S. Atomic Energy Commission.

addition, a more rapid decompression of the pellet occurs during thermonuclear burn which results in a decrease in yield ratio.

Adiabatic compression is desired to minimize the pressure needed for compression and to remain near the Fermi-degenerate pressure this keeping the transport of energy small compared to the Fermi energy. This condition is achieved by making the coupling efficient between the laser heated electrons and the electrons inside the critical radius.

This problem of an energetic electron tail, of the form

$$F(v) = Bv^2 \exp(-\frac{1}{2} mv^2/\alpha kT_e),$$

can be reduced if not eliminated by limiting the laser intensity (laser power divided by area of critical surface) to values below the threshold estimates for the plasma instabilities. The estimated value for threshold varies in a fashion similar to the nation's economy with about the same time constant. For the purposes of this study it will be assumed to be 1×10^{13} watts/cm^2 in DT at an electron temperature of 1 keV for 1 μm light.

Another factor enters into threshold considerations. The threshold is proportional to the "swelling factor" (which corrects for the increasing electromagnetic field as the light approaches the critical density) thus reducing the threshold intensity by a factor of 10 or so. This may be regained by the bandwidth effects of the laser (an FM modulation). Hence in these calculations these two effects will be considered to cancel each other.

PELLET GEOMETRY AND ITS RATIONAL

Figure 2 shows the configuration of a pellet which overcomes the problem of generating superthermal electrons. A hollow DT sphere of 60 μg is surrounded by 80 μg of solid Ne which is in turn surrounded by a low density DT atmosphere that might be produced by a laser prepulse. The atmosphere is divided into two regions such that the innermost region is slightly above the critical density for 2 μm light.

The radii of the DT sphere is chosen for a $r/\Delta r$ of 10 : 1 which reduces the maximum ablation pressure (and laser power) required to achieve the necessary implosion velocity, and the number of changes of wavelength of light. The thinness of this shell places some requirements on the surface finish as will be discussed later.

The medium-z coating surrounding the DT is used for two reasons: there is more shielding of the DT from energetic electrons since the mean-free-path in this material is reduced by a factor of z^2; and, the plasma instability threshold is raised and is proportional to $\overline{z^2}/\bar{z}$. For the Ne coating used here the threshold is raised by a factor of 10. The thickness of Ne was chosen so that the ablation front had not reached the DT sphere at the time of ignition for the shortest wavelength used (1/2 μm).

NUMERICAL SIMULATION OF THE IMPLOSION

The implosion of many pellet configurations and laser pulse shapes have been simulated with the hydrotransport and thermonuclear burn code LASNEX[2].

Both intensity and wavelength shaping of the laser pulse are used starting with 2 μm light and frequency doubling to 1/2 μm light. The 2 μm light is required to achieve a few percent uniformity in ablation pressure at early times while the 1/2 μm light is required to minimize the electron de-coupling at late times and high laser powers. The use of the 1/2 μm light allows a higher light intensity (and hence power) to be used since the plasma instability threshold is

$$I \sim \left(\frac{N_e{}^3}{T_e}\right)^{1/2} \frac{\overline{z^2}}{\overline{z}}$$

The procedure used was to begin with the given mass of DT and incorporate enough Ne to insure burn-through to the DT was not achieved for 1/2 μm light. This geometry was then used for 2 μm light and a temporal pulse shape was found which produced a significant yield ratio ($\gtrsim$ 15:1). A point on the laser power curve was selected to be slightly below the threshold intensity and a 1 μm pulse was impressed and carried to ignition with a slightly better yield ratio ($\gtrsim$ 20:1). Again the process was repeated with 1/2 μm light to give the overall implosion. These were one-dimensional and three-temperature (electron, ion, radiation) problems. Figure 3 presents the pulse shapes used. All temporal shapes behave according to[3]

$$\dot{E}(t) = \dot{E}_0 \left(1 - \frac{t}{T}\right)^{-100}$$

Figure 4 is the impressed laser intensity for the three wavelengths as a function of time together with the instability thresholds.

The 2 μm light was deposited entirely in the DT atmosphere and was taken to a power of 6.5 X 10^{11} watts. The 1 μm light has its critical density within the Ne and the initial power was adjusted to approximately match the pressure from the 2 μm pulse at a point within the DT shell. A final 1 μm power of 1.1 X 10^{13} watts was reached when the 1/2 μm light was initiated. The final laser power used resulted in an intensity slightly above threshold.

Additional calculations have been made using a multi-group radiation distribution. The effect of this distribution is shown in Fig. 5 where the pressure-density relation is plotted for a central zone. It is seen that the photon distribution, which arises from free-bound and free-free collisions, causes the compression to proceed along a higher adiabat resulting in a lower yield.

Near the end of the implosion, the inside portion of the Ne has a temperature of several keV thus causing this material to radiate into the DT. The result is similar to that from electron preheat or the multi-group radiation spectrum in that the compression is forced to a higher adiabat. Figure 6 plots the radiation and material temperatures as a function of time while Fig. 7 plots the density and pressure for a given fuel zone. As a consequence the outer portion of DT is underdense to the alpha particles and approximately 65% of the DT is not consumed in thermonuclear burn.

SYMMETRY AND STABILITY OF THE IMPLOSION

Hollow DT shells are particularly succeptible to Taylor instability. The following paper will present a detailed analysis of the growth of surface perturbations. At the time of preparation of this paper, the calculations have not been optimized, but their results suggest that a continuous pulse of the type used here is not proper for realistic surface defects.

CONCLUSIONS

The use of a hollow pellet of high $r/\Delta r$ permits the successful generation of thermonuclear energy for a moderate laser input. Incorporation of a medium-z material is required for minimization of plasma instabilities and thus suppression of pathelogically hot electrons. Designs of this nature are capable of giving yield ratios in excess of 20 for 100 kJ input.

It is also likely that a lower-z material may be advantageous to minimize the x-rays radiation into the DT, but this will be at the sacrifice of using less laser power to remain below the plasma instability threshold.

REFERENCES

1. J. D. Lindl, LLL Report UCRL-74928, October, 1973.

2. G. B. Zimmerman, LLL Report UCRL-74811, October, 1973.

3. A. R. Thiessen, LLL Report UCRL-74923, October, 1973.

Figure 1:	Effect of superthermal electrons on pressure required to achieve a high compression in DT.
Figure 2:	Initial material configuration.
Figure 3:	Power and wavelength time dependence for laser sources. First pulse is employed to create a hot atmosphere surrounding pellet to improve coupling of subsequent light to the pellet.
Figure 4:	Laser intensities and plasma instability thresholds for the laser sources.
Figure 5:	Pressure-density relation for two types of photon transport.
Figure 6:	Effect of radiation on material temperature in DT fuel.
Figure 7:	Time history of compression in DT fuel.

PRESSURE VS. DENSITY FOR A CENTRAL DT FUEL ZONE

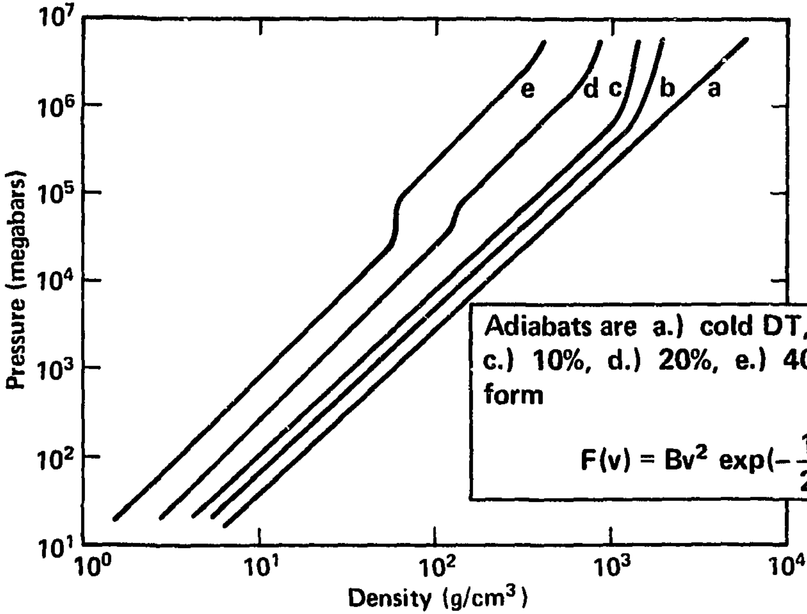

Adiabats are a.) cold DT, b.) 0% superthermal electrons, c.) 10%, d.) 20%, e.) 40%. Superthermal tail is of the form

$$F(v) = Bv^2 \exp(-\frac{1}{2} mv^2/\alpha k T_e)$$

FIGURE 1

SECTION OF THE CONCENTRIC MATERIAL PELLET USED IN THE PULSE SHAPE INVESTIGATIONS

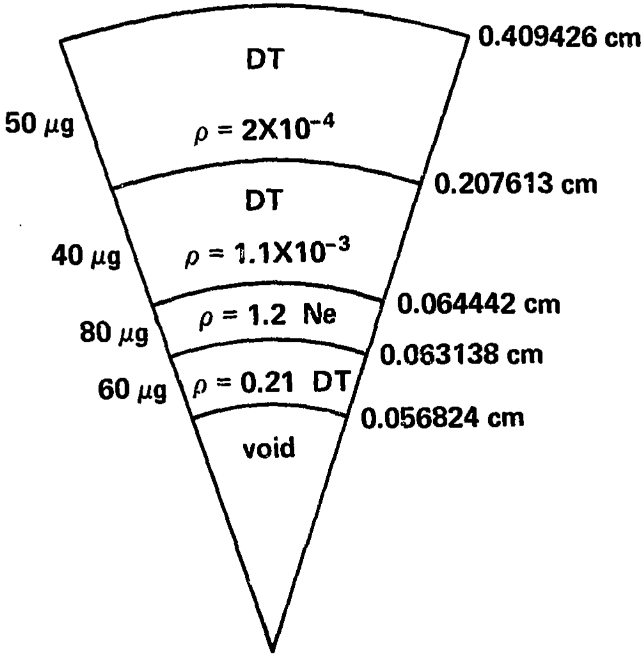

FIGURE 2

LASER PULSE SHAPES

Each wavelength has the temporal shape $\dot{E}(t) = \dot{E}_0 (1 - \frac{t}{\tau})^{-100}$

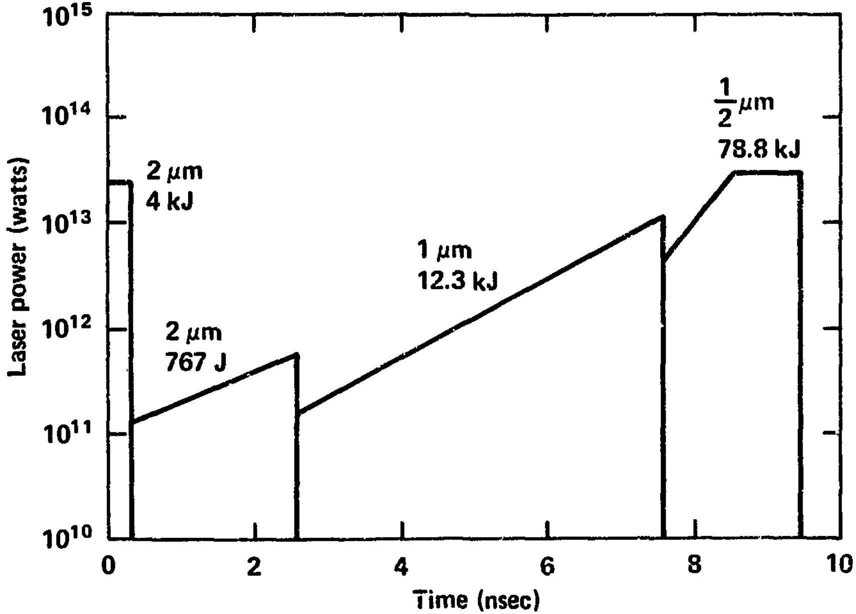

FIGURE 3

LASER INTENSITIES (SOLID LINES) AND PLASMA INSTABILITY THRESHOLDS (SEMI-SOLID LINES) FOR THE THREE WAVELENGTHS USED

Dashed lines are times when wavelengths are changed

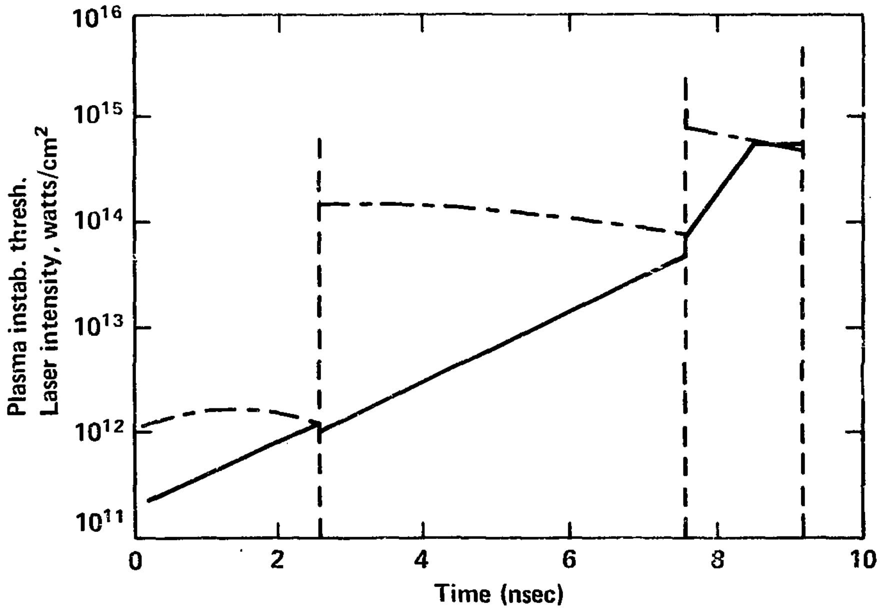

FIGURE 4

EFFECT OF THE MULTI-GROUP PHOTONICS (DASHED LINE) AND SINGLE RADIATION TEMPERATURE (SOLID LINE) PHYSICS ON ISOTHERMAL COMPRESSION

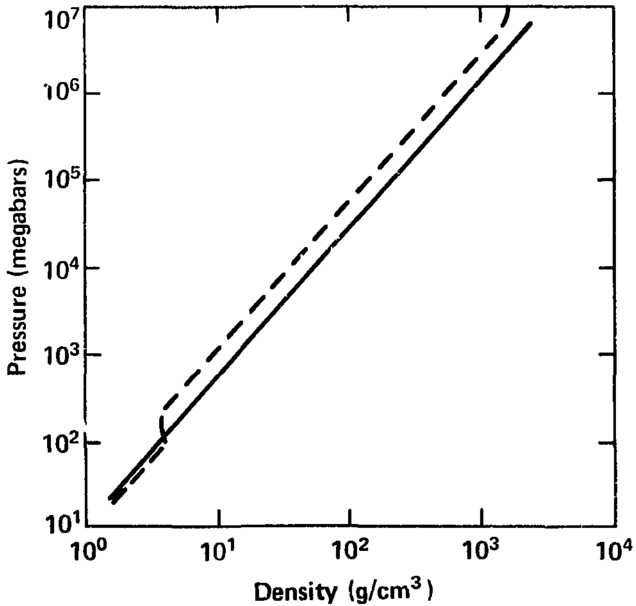

FIGURE 5

RADIATION FIELD AND MATERIAL TEMPERATURES FOR A CENTRAL FUEL ZONE

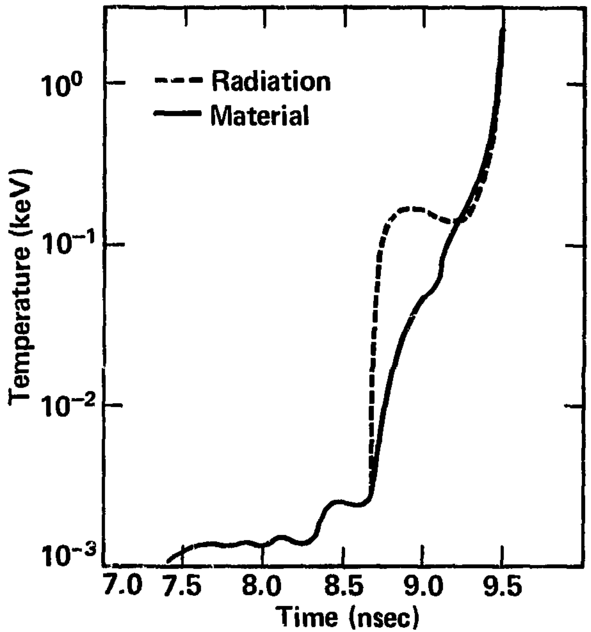

FIGURE 6

PRESSURE (DASHED LINE) AND DENSITY (SOLID LINE) FOR A CENTRAL FUEL ZONE

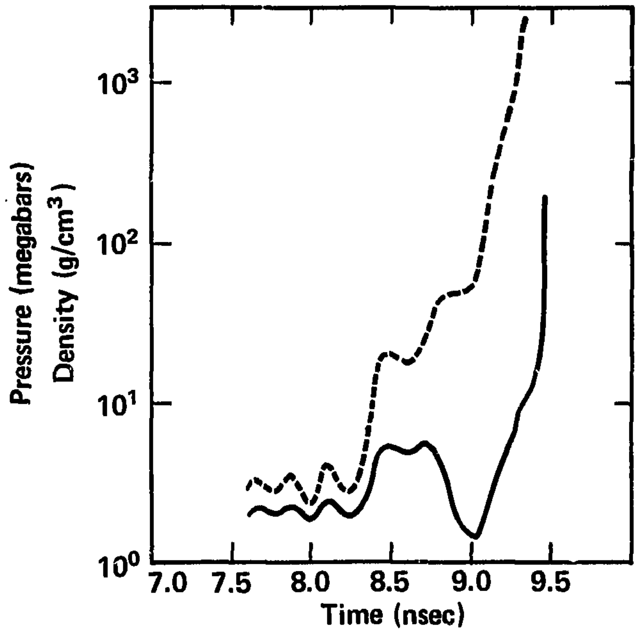

FIGURE 7